PCCP

Accepted Manuscript

ROYAL SOCIETY OF CHEMISTRY

www.rsc.org/pccp

Journal Name

RSCPublishing

ARTICLE

Probing the Ligand Recognition and Discrimination Environment of the Globin-Coupled Oxygen Sensor Protein YddV by FTIR and Time-Resolved Step-Scan FTIR Spectroscopy

Cite this: DOI: 10.1039/xoxxoooooox

Received ooth January 2012,
Accepted ooth January 2012

DOI: 10.1039/xoxxoooooox

www.rsc.org/

Andrea Pavlou,[a] Markéta Martínková,[b] Toru Shimizu,[b] Kenichi Kitanishi,[b] Martin Stranava,[b] Andreas Loullis,[a] Eftychia Pinakoulaki[a,*]

YddV is a newly discovered signal transducer heme protein that recognizes O2 and CO. Structural differences in the ligand-bound heme complex in YddV reflect the variations in catalytic regulation by O2 and CO. Time-resolved step-scan (TRS^2) FTIR studies of the wild type and of the important in oxygen recognition and stability of the heme Fe(II)-O2 complex L65M, L65T, Y43A, Y43F and Y43W mutants were performed to determine the site-specific protein dynamics following carbon monoxide (CO) photodissociation. These mutations were designed to perturb the electrostatic field near the iron bound gaseous ligand (CO), and also to allow us to investigate the communication pathway between the distal residues of the protein with the heme. The TRS^2-FTIR spectra of YddV-heme-CO show that the heme propionates are in the protonated and deprotonated state. Moreover, the rate of decay of the amide I vibrations is on a time-scale coincident with the rate of rebinding of CO suggesting that there is a coupling between ligation dynamics in the distal heme environment and (i) the protein backbone relaxation and (ii) the environment sensed by the heme propionates. The fast recombination rates in L65M, L65T and Y43W implies significant role of L65 and Y43 in controlling the ligand dynamics. The implications of these results with respect to the role of the heme propionates and the charged or proton donating residues in the distal pocket that are crucial for stabilizing the bound gaseous ligands are discussed.

Introduction

In the *Escherichia coli* geneome, *yddV* and *dos* genes are organized as a bicistronic operon to regulate synthesis and degradation of 3′-5′-cyclic diguanylic acid (c-di-GMP), respectively.[1] Modulation of overall conversion from GTP to pGpG via c-di-GMP is catalyzed by YddV (also termed *Ec*DosC) and *Ec*DOS (*Escherichia coli* direct oxygen sensor, also termed *Ec*DosP). The *dos* gene product is the heme-based oxygen sensor protein *Ec*DOS and the *yddV* product from *Escherichia coli* (*Ec)* is a globin-coupled heme based oxygen sensor protein displacing diguanylate cyclase activity in response to oxygen availability.[1-3] The globin-coupled oxygen sensor protein structures and signal transduction mechanisms are unique and differ from those of FixL and *Ec*DOS, which contain the heme bound PAS fold domain.[2-7] The sensor domain of the globin-coupled oxygen sensor family has a globin fold at the N-terminus and contains a heme that acts as the O_2-binding site, but with limited amino acid homology to myoglobin (Mb) and hemoglobin (Hb), and the diguanylate cyclase (DGC) domain at the C-terminus. The globin fold lacks the D and half of the E-helices of Mb and Hb. Seven heme-based oxygen sensor proteins with the globin fold, YddV, *Af*GcHK, HemAT-*Bs*, HemDGC, *Bpe*GReg, *Av*GReg, and *Gs*GCS are known to date.[2,3,7-13] Because of the importance of c-di-GMP as messenger in bacteria and the increasing interest in understanding the connectivity between O_2 and the metabolism of c-di-GMP,[14] it is essential to elucidate the properties of the newly discovered globin-coupled oxygen sensor proteins. In addition, little is known about the dynamics of signal transduction by globin-coupled oxygen sensors and the role of the distal environment in regulating the binding of

O_2 and CO. Determination of the structural dynamics of the protein moiety associated with the ligand binding/photo-dissociation from bound ligand(s) to the heme Fe(II) is of particular importance towards our interest in understanding the initial steps in the signalling mechanism.

Of the known globin-coupled oxygen sensors crystal structures have been reported for the sensor domain of HemAT from *B. subtilis* (HemAT-*Bs*) and *Gs*GCS.[8,12] The sensor domain of HemAT-*Bs* is a homodimer with significant differences in the conformation of the distal residues (A91, T95, V89, Y70) surrounding the heme in each subunit.[8] HemAT detects O_2 in the sensor domain and transmits the signals through conformational changes to its functional domain showing the activity associated with the methyl-accepting chemotaxis. Resonance Raman (RR) studies revealed the formation of open and closed forms of six-coordinate O_2-bound HemAT-*Bs*, suggesting the involvement of the distal residue T95 in regulating O_2 binding through the observed H-bond formation with the heme coordinated O_2;[15] the other distal residues are Y70, L92, R91 and V89. In addition, the formation of H-bonds between the proximal ligand H86 to the heme iron with the heme 6-propionate and between T95 and heme bound O_2 results in conformational changes in the E and B-helices.[16] On the other hand, based on the observation that mutation of Y70 made the dissociation constant of the heme-bound O_2 larger than the wild type, it was proposed that Y70 forms a H-bond with the bound to the heme O_2,[17] in contrast to the conclusions based on the RR experiments.[15] In addition, the UV Raman experiments indicated a change to a more hydrophilic environment around Y70 in the ligand-bound forms, without the formation of a H-bond between Y70 and O_2 or CO.[18] Interestingly, it has also been proposed that the O_2-bound form has a structural linkage with the signaling domain and that negative cooperative or heterogeneity play a key role in the signal transduction pathway.[17] The different conclusions on the role of Y70 to the binding and recognition of the O_2 signaling ligand, which were based on different experimental approaches, leave open questions. Recently, it was demonstrated that although the heme cavity recognizes ligands such as O_2, NO and CO, the conformational changes induced in the protein distal site are not similar, and only O_2 alters the distal site in such a way that the conformational changes are transmitted to the effector domain.[18]

Based on the catalytic activities in terms of the initial rate of product formation (c-di-GMP) similar turnover numbers (0.022 min^{-1}) were measured for O_2 and CO indication that YddV recognizes both O_2 and CO.[3] In the absence of x-ray crystallographic data based on the comparative amino acid sequence study with well-known heme-based sensors it has been proposed that H98 is the proximal to the heme ligand. The isolated sensor domain YddV (YddV-heme) forms only five-coordinate high spin Fe(III) complex containing a proximal H98 as the fifth ligand.[3] On the distal site it has been demonstrated that the conserved residues L65 and Y43 are important for the binding and stabilization of the heme Fe(II)-O_2 complex.[3,19,20] Extensive pH studies on L65 mutant proteins have revealed the presence of H_2O molecule as the sixth axial ligand, which is converted to OH^- at alkaline pH, and the formation of a six-coordinated low-spin species.[19] RR Soret excitation experiments of wild type and Y43F mutant protein, have been reported.[3] The RR frequencies of the wild type protein of the oxy complex with ν(Fe-O_2) =565 cm^{-1} and CO complex with ν(Fe-CO) = 495 cm^{-1} are distinctly different from those reported at ν(Fe-O_2)=559 cm^{-1} and ν(Fe-CO)= 505 cm^{-1} for the Y43F mutant protein, suggesting that Y43 forms a H-bond with the bound to the heme iron O_2 and CO ligands. Interestingly, the Y43A and Y43L mutant proteins exhibited very low O_2 affinities, and thus, the ν(Fe-O_2) was not observed. In addition, the ν(CO) for the wild-type and Y43F mutant protein were reported at 1965 and 1959 cm^{-1}, respectively, indicating the formation of a single conformation.[3]

Fourier transform infrared (FTIR) spectroscopy has been extensively applied to monitor the distal to the heme environment of the heme-bound CO ligand and time-resolved step-scan FTIR (TRS^2-FTIR) spectroscopy has proven to be very powerful technique in studying transient changes at the level of individual amino acids during protein action and conformational changes of the protein backbone.[21-27] YddV is a globin-coupled heme based oxygen sensor protein in which critical roles in O_2 and CO recognition have been reported for Y43 and L65 residues and thus, in this work we have applied FTIR and TRS^2-FTIR to probe the dynamics of wild type YddV-heme as well as of different Y43 and L65 mutants of the protein. In the FTIR spectrum of the CO-bound YddV-heme we detect two CO modes at 1962 and 1923 cm^{-1}, which we attribute to neutral and strong H-bonded conformers, respectively. In the spectra of the L65M mutant a single vibration of the C-O is observed at 1953 cm^{-1} indicating strong alteration in the distal structure upon the L65M mutation. On the other hand, although the CO adduct of the L65T mutant produced a low photoproduct yield (29%), the CO vibration was observed at the same frequency as the wild type at 1962 cm^{-1}, suggesting that the L65T mutation makes no significant alterations in the interactions of the bound CO with the distal environment. Both the Y43A and Y43W mutants produced photoproduct yields similar to that observed in the wild type protein (>90%), but the C-O mode is observed at 1962 and 1953 cm^{-1}, respectively. The Y43F mutant produced low photoproduct yield and the C-O mode at 1955 cm^{-1}. The TRS^2-FTIR difference spectra of wild type YddV-heme-CO subsequent to CO photodissociation show that the heme propionates are in the protonated and deprotonated forms and the observed constant for CO recombination to the heme iron is k_{WT}= 528 s^{-1} at pD 8. Perturbation of the amide I is observed upon CO photolysis. The rate of decay of the amide I and heme propionates vibrations is on a time-scale coincident with the rate of CO rebinding suggesting that there is a coupling between ligation dynamics in the distal heme environment and (i) protein relaxation and (ii) the environment sensed by the heme propionates. Based on the observed recombination constants for the L65 and Y43 mutants we conclude that rebinding is faster in the L65 mutants than in the Y43 mutants.

Materials and Methods

Materials

All chemicals used were of the highest purity grade available from commercial sources and used without further purification. Potassium phosphate was obtained from Sigma-Aldrich (St. Louis, MO, USA). Water, doubly distilled over quartz, was purified using a Milli-Q Plus system (EMD Millipore, Billerica, MA, USA). All glassware used for sample preparation was conditioned in advance by standing for 24 hr in 10% HCl suprapur (Merck, Darmstadt, Germany).

Overexpression and protein purification

Cloning, site-directed mutagenesis, overexpression in *E. coli* and purification of YddV-heme were performed as previously described.[3,19,20] The WT and Y43F, Y43L, Y43W, L65M, L65T mutants of YddV-heme were prepared as described below. Briefly, *E. coli* BL21(DE3) (Stratagene, Novagen) was transformed with the appropriate plasmid (pET28a(+)/YddV-heme-Histag), plated on LB agar containing kanamacin (50 mg/ml) and incubated at 37 ^{o}C overnight. On the following day, a single colony was inoculated in TB medium containing kanamycin and shaken overnight at 250 rpm and 37 °C. The culture medium was then added to fresh TB medium (1:200 dilution) containing kanamycin and the mixture was again shaken at 250 rpm and 37 °C. Once the culture reached an OD600 of 1.2, the medium was cooled to 20 °C and protein expression was induced by the addition of 0.1 mM isopropyl β-D-thiogalactopyranoside and 0.45 mM δ-aminolevulinic acid, followed by further shaking for 24 hrs. The *E. coli* cells were harvested by centrifugation for 30 min at 5,000 g and 4 °C, frozen in liquid nitrogen, and stored at -80 °C until protein extraction and purification. Frozen pellet cells were suspended in buffer A [50 mM Tris-HCl pH 8.0, 150 mM NaCl, 20 mM imidazole] containing 1 mM phenylmethanesulfonyl fluoride (PMSF) and lysed with 0.2 mg/ml lysozyme. The crude extract was sonicated and then centrifuged at 25,000g for 1 hr. The resulting supernatant was applied to a His Trap HP column (GE Healthcare, Amersham, U.K.) that had been pre-equilibrated with buffer A containing PMSF. The recombinant proteins were retained due to their $(His)_6$ tags and then eluted using a linear gradient from 20 to 300 mM imidazole in buffer A. Protein fractions were pooled and dialyzed against a 50 mM pH 8.0 Tris-HCl buffer overnight. Finally the purified proteins were quickly frozen in liquid nitrogen and stored at -80 °C.

UV-Vis spectroscopy

Optical absorption spectra were recorded with a Shimadzu UV1700 UV-visible spectrometer. A 2 µl sample of wild type YddV-heme was diluted into 300 µl of 50 mM Tris-HCl buffer pH 8 to achieve a final concentration of about 8 µM. The reduction of YddV was carried out under anaerobic conditions by adding a few grains of sodium dithionite into Tris buffer and then ~3 µl in the YddV-heme sample. For the preparation of the carbonmonoxy adduct, dithionite-reduced sample was exposed to 1 atm of CO (1 mM) in an anaerobic sealed quartz cuvette of path length 1 cm. Optical absorption spectra were also recorded before and after the FTIR measurements to ensure the formation and stability of the CO adducts.

Sample preparation for FTIR measurements

The YddV-heme samples used for the FTIR measurements had a concentration of~0.7-1.0 mM in 50 mM Tris for pH 8 and pD 8 after buffer exchange. The pD solutions prepared in D_2O buffers were measured by using a pH meter and assuming pD = pH (observed) + 0.4. Dithionite reduced samples were exposed to 1 atm of CO in an anaerobic cell to prepare the carbonmonoxy adduct and transferred to a tightly sealed FTIR cell with two CaF_2 windows, under anaerobic conditions (path length (l)= 6 µm). CO gas was obtained from Linde.

FTIR and TRS^2-FTIR measurements

The static FTIR spectra were recorded with 4 cm^{-1} spectral resolution on a Bruker Vertex 80V spectrometer. For the time-resolved step-scan FTIR measurements, the 532 nm pulses from a Continuum Minilite II Nd:YAG laser (5 ns width, 10 Hz) were used as a pump light (4 mJ/pulse) to photolyze the YddV-heme-CO adducts. A vacuum pump was used to evacuate the interferometer compartment to a final pressure of 3.2 mbar. The FTIR spectrometer was placed on a Newport VH optical vibration isolation table to ensure that vibrational background noise from environmental sources was avoided. For the time- resolved experiments, a TTL (transistor transistor logic) pulse provided by a digital delay pulse generator (Quantum Composers, 9524) triggered in order the flashlamps, the Q-switch, and the FTIR spectrometer. Pretriggering the FTIR spectrometer to begin data collection before the laser fires allows fixed reference points to be collected at each mirror position. Changes in intensity were recorded with a photovoltaic MCT detector (Kolmar Technologies KV100-1B-7/190, response limit 850 cm^{-1}) and digitized with a 180-kHz, 24-bit, analog-to-digital converter (ADC). A broadband interference optical filter (LP-4200, Spectrogon) with a short wavelength cutoff at 4.2 µm was used to limit the free spectral range from 4.2 to 11.8 µm. This led to a spectral range of 2633 cm^{-1}, which was equal to an undersampling ratio of 6. Single-sided spectra were collected at 4 cm^{-1} spectral resolution, 6 µs time resolution, and 10 coadditions per data point. The total accumulation time for each measurement was 25 min, and 15 measurements were collected and averaged. Blackman-Harris three-term apodization with 32 cm^{-1} phase resolution and the Mertz phase correction algorithm were used. The photoproduct yield at 6 µs was calculated by dividing the ΔA of the CO mode in the TRS^2-FTIR spectrum at 6 µs with that in the FTIR spectrum recorded prior to the photodissociation experiment.

Results and Discussion

Fig. 1 shows a schematic presentation of the heme site of CO-bound YddV. The optical absorption spectrum of Fe(III) as isolated YddV-heme shown in Fig.2 (trace A) displays Soret maxima at 394 nm and visible (Q-band) band at 506 nm, which is typical of a five-coordinated, high spin Fe(III) heme protein. The latter confirms the hitherto reported,[3] distinctive structural architecture of Fe(III) YddV as a 5-coordinated high spin globin coupled sensor compared to other GCS, which appear as 6-coordinated low or high spin in the Fe(III) form and provides evidence that there is no axial water or OH^- coordinated to the heme-Fe(III). In addition, a shoulder at 642 nm is observed that is typical of a porphyrin-to-ferric iron charge transfer (CT) transition characteristic of ferric high spin heme *b* (Fig. 2, *trace A*). The dithionite reduced YddV-heme protein, shown in Fig. 2 *trace B*, displays Soret maxima at 432 nm and a visible band at 560 nm, indicating the formation of a 5-coordinated high-spin complex. Upon exposure of the reduced protein to 1 atm of CO gas, a spectrum shown in Fig. 2C with a Soret maximum at 421 nm and visible bands at 540 and 566 nm was obtained. The spectrum of the Fe(II)-CO complex indicates the formation of a six-coordinated low-spin species, as shown previously.[3]

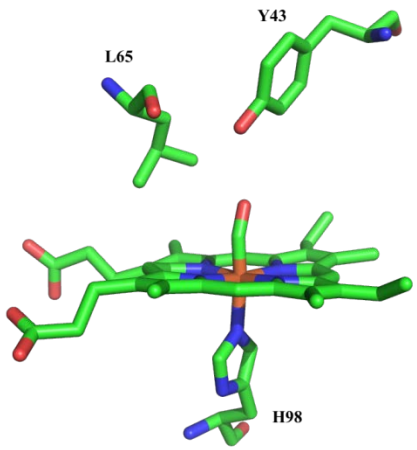

Fig. 1. Schematic representation of the proposed structure of the CO-bound form of YddV (residues are numbered for YddV), based on the crystal structure of Fe(III)-CN adduct of HemAT-*Bs* (PDB 1OR4)[8] and homology modeling.

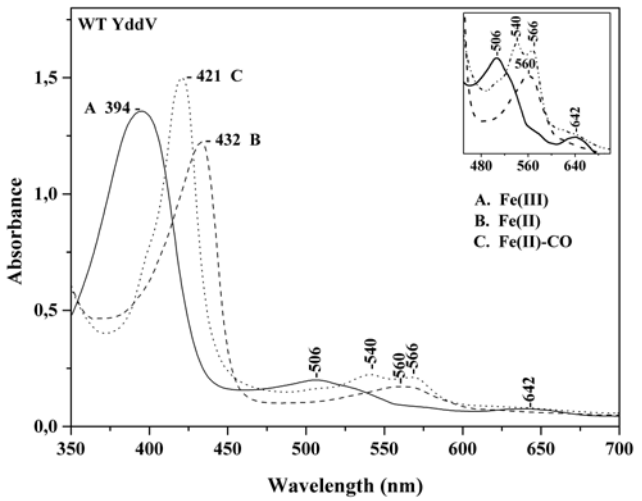

Fig. 2. Optical absorption spectra of wild-type YddV-heme at pH 8. Trace A (solid line) is the Fe(III), trace B (dashed line) is the Fe(II) form, and trace C (dotted line) is the Fe(II)-CO form. The enzyme concentration was 8 µM, and the path length was 1 cm.

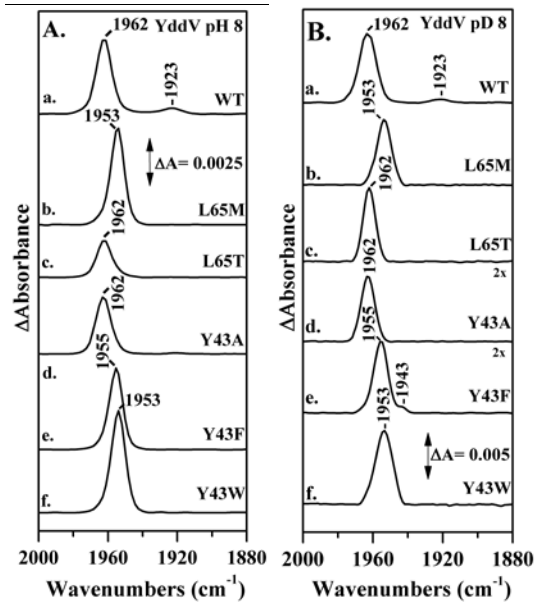

Fig. 3. FTIR spectra of the YddV-heme-CO adducts at (**A**) pH 8 and (**B**) pD 8 representing wild type YddV (trace a), and L65M (trace b), L65T (trace c), Y43A (trace d), Y43F (trace e), and Y43W (trace f) mutants. The pathlength was 6 µm and the spectral resolution was 4 cm^{-1}.

We detect two modes at 1962 and 1923 cm^{-1} in the FTIR spectrum of the $^{12}C^{16}O$-bound YddV-heme (Fig. 3A *trace a*); both are sensitive to the isotopic substitution of CO and downshift to 1918 and 1878 cm^{-1}, respectively, when the experiment is performed using the isotopically labelled $^{13}C^{16}O$ (Fig. 1, ESI). We assign the ν_{CO} of YddV-heme based on the ν_{CO} of Mb observed at 1910-1930 cm^{-1} (strong H-bonding interaction), 1940-1950 cm^{-1} (moderate H-bonding interaction) and 1960-1970 cm^{-1} (neutral).[21] Therefore, we assign the major band in the FTIR spectrum of the CO-bound YddV-heme at 1962 cm^{-1} (neutral) and the minor band (strong H-bonding interaction) at 1923 cm^{-1} to the C-O modes of the heme Fe(II)-CO complex. The detection of the major band has been reported in the RR spectra (ν_{CO}=1965 cm^{-1}),[3] but the strong H-bonding conformer is reported for the first time. Similar open (neutral) and closed (H-bonded) conformers have also been reported for CO-bound HemAT.[28,29] In the spectra of the L65M (Fig. 3A, *trace b*) mutant the C-O modes are observed at 1953 cm^{-1}, which is 9 cm^{-1} lower than that observed in the wild type indicating strong alteration in the distal structure upon the L65M mutation. On the other hand, in the L65T mutant (Fig.3A, *trace c*) the C-O mode was observed at the same frequency as the wild type at 1962 cm^{-1}, suggesting that the L65T mutant makes no significant alterations in the interactions

of the bound CO with the distal environment. In the Y43F (Fig. 3A, *trace e*) and Y43W mutants (Fig. 3A, *trace f*) the C-O mode is observed at 1955 and 1953 cm^{-1}, respectively, but in the Y43A mutant (Fig. 3A, *trace d*) the C-O mode is observed at the same frequency as the wild type. Noticeably, in none of the mutant proteins examined the strong H-bonding conformer observed in the wild type at 1923 cm^{-1} was detected.

We have investigated the CO-bound YddV-heme complex at pD 8, aiming to explore the pH/pD sensitivity of the distal site in the YddV-heme-CO complex (Fig. 3B). The observed pD sensitivity includes the decreased intensity of the strong H-bonding conformer at 1923 cm^{-1} (Fig. 3B, *trace a*) and broadening of the CO peak in the Y43W mutant (Fig. 3B, *trace f*) that indicates the involvement of multiple protein-ligand conformations differing in the polarity of electrostatic interactions. In addition, a moderate hydrogen bonded conformer was observed at 1943 cm^{-1} in the Y43F mutant (Fig. 3B, *trace e*). The rest of the data in D_2O for all proteins examined are similar to those observed at pH. The absence of the strong H-bonding conformer in the L65 and Y43 mutant proteins demonstrates that both residues significantly perturb its formation. The insensitivity of the CO mode of the major conformer in the L65T and Y43A mutant proteins indicates, in contrast to those for L65M, Y43W and Y43F, that these specific mutations are not directly involved in controlling the strength of the C-O bond.

Fig. 4A and 4C show the TRS^2-FTIR difference spectra (t_d= 6 μs-7.4 ms, 4 cm^{-1} spectral resolution) of YddV-heme at pD 8 subsequent to CO photolysis in different spectral regions. The negative band at 1962 cm^{-1} in Fig. 4A originates from the photolyzed heme-CO complex (92% photoproduct yield at 6 μs), while the 1923 cm^{-1} conformer is not observed in the TRS^2-FTIR spectra presumably due to its much weaker intensity. The continuous variability in the intensity of the CO mode associated with heme iron over a 6 μs-7.4 ms time scale is used to quantify ligand rebinding to the heme. The final spectrum at 7.4 ms demonstrates that there is no irreversible light-induced effect on the heme iron. The intensity of Fe(II)-CO band at 1962 cm^{-1} was measured as a function of time to determine the rate of recombination of CO to the heme iron (k =528 s^{-1}) at room temperature (Fig. 4B). The curve is a three parameter fit to the experimental data according to pseudo first-order kinetics. In the FTIR difference spectra obtained upon CO-photolysis from the heme iron, the appearance of signals in the amide I region (1620-1680 cm^{-1}) can be attributed to changes of the C=O modes caused by perturbation in the polypeptide backbone with possible contributions from Gln/Asn side chains.[30] The asymmetric COO^- modes from deprotonated heme propionates and Glu and Asp side chains are expected in the 1530-1590 cm^{-1} region.[27,30-32] The presence of the positive peak at 1670 cm^{-1} in the time-resolved step-scan FTIR spectra of the YddV-heme-CO adduct subsequent to CO photodissociation (Fig. 4C) can be tentatively assigned to the protonated form of the heme propionates indicating that the propionates are perturbed upon CO photodissociation.[31] We attribute the peaks/troughs at 1646/1656 cm^{-1} to amide I

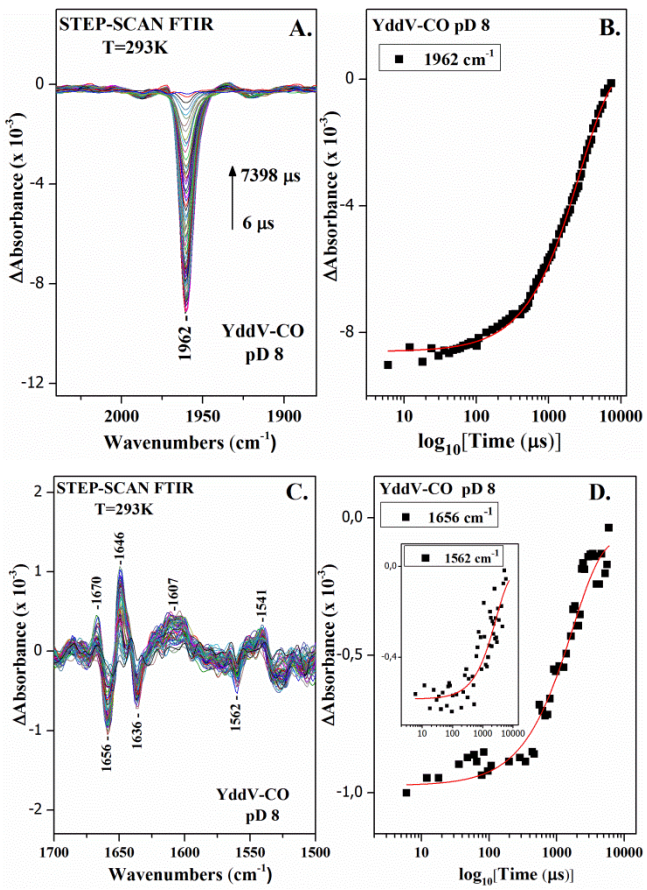

Fig. 4. (A) Time-resolved step-scan FTIR difference spectra of the wild type YddV-heme-CO adduct at pD 8 from 6 to 7398 μs subsequent to CO photolysis. **(B)** Plot of the ΔA of the 1962 cm^{-1} mode versus time on a logarithmic scale subsequent to CO photolysis. **(C)** Time-resolved step-scan FTIR difference spectra of the wild type YddV-heme-CO adduct at pD 8 in the 1700-1300 cm^{-1} range and t_d = 6 – 7398 μs. **(D)** Plot of the ΔA of the 1656 cm^{-1} mode versus time on a logarithmic scale subsequent to CO photolysis. The red lines correspond to the exponential fitting of the experimental data. The inset includes the plot of the ΔA of the 1562 cm^{-1} mode versus time on a logarithmic scale subsequent to CO photolysis.

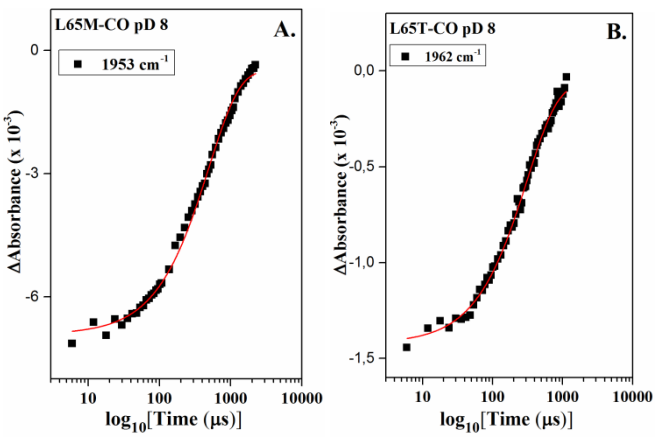

Fig. 5. Plot of the ΔA of the 1953 cm^{-1} mode of L65M YddV-heme-CO **(A)** and 1962 cm^{-1} mode of L56T YddV-heme-CO **(B)** versus time on a logarithmic scale subsequent to CO photolysis. The red lines correspond to the exponential fitting of the experimental data.

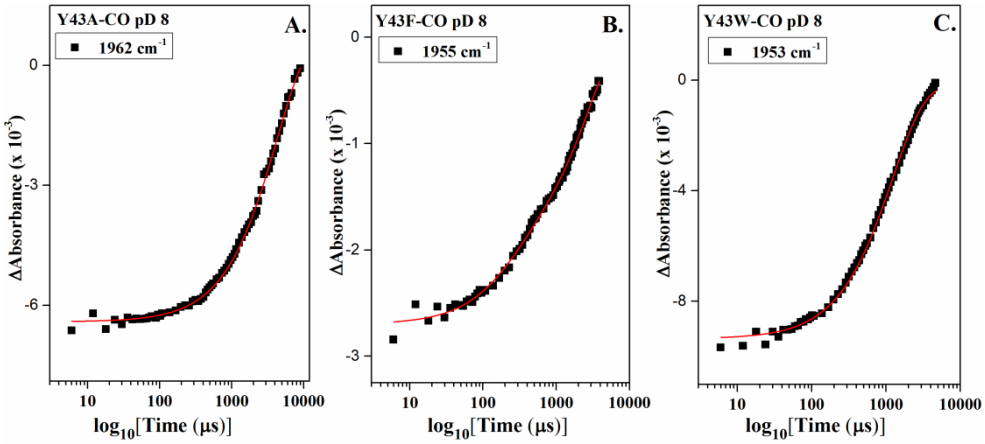

Fig. 6. Plot of the ΔA of the 1962 cm^{-1} mode of Y43A YddV-heme-CO **(A),** of the 1955 cm^{-1} mode of Y43F YddV-heme-CO **(B)** and of the 1953 cm^{-1} mode of Y43W YddV-heme-CO **(C)** versus time on a logarithmic scale subsequent to CO photolysis. The red lines correspond to the exponential fitting of the experimental data.

Table 1. Time and rate constants for CO rebinding and % photoproduct yield at 6 μs for the wild type and mutant YddV-heme-CO adducts.

	t_1 (μs)	k (s^{-1})	% photo-product at 6 μs
WT	1312 ± 73	528	92
L65M	393 ± 13	1764	91
L65T	237 ± 8	2929	29
Y43A	2424 ± 92	285	92
Y43F	1363 ± 32	508	34
Y43W	845 ± 22	820	92
Amide I (WT)	1443 ± 179	480	
Heme prop. (WT)	1461 ± 479	474	

absorbance and the 1541/1562 cm^{-1} pair to the $\nu(COO^-)^{asym}$ of propionate(s).[27,30-32] The intensity of the amide I mode at 1656 cm^{-1} (Fig. 4D) and of the heme propionate(s) mode at 1562 cm^{-1} (inset, Fig. 4D) was measured as a function of time and the corresponding rate constants (k_{1656} = 480 s^{-1} and k_{1562} = 474 s^{-1}) were calculated as described previously for the CO mode. Thus, the amide I and heme propionate(s) modes follow similar kinetics with CO rebinding. Intensity changes and/or frequency shifts at 1636 cm^{-1} that could be attributed to Gln or Asn are present in the TRS^2-FTIR spectra.[30]

In an effort to elucidate the environment sensed by the bound CO, we have investigated the TRS^2-FTIR of the CO-adducts of L65M (Fig. S2A, ESI) and L65T (Fig. S2B, ESI) YddV mutants, and Y43A (Fig. S3A, ESI), Y43F (Fig. S3B, ESI) and Y43W (Fig. S3C, ESI) mutant proteins subsequent to CO photolysis. The intensity of Fe(II)-CO bands were measured as a function of time to determine the rate of recombination of CO to heme iron in each mutant (Fig.5 and Fig. 6). The rate of recombination of CO to heme iron in the wild type YddV-heme and mutant proteins as well as the yield of photoproduct formation at 6 μs are summarized in Table 1. A close inspection of the data shows the large effect of the L65M and L65T mutants of YddV-heme protein on the recombination of CO. Both the ligand association rate constant and the ligand rebinding rate constant reflect the environment of the ligand access to the binding site. In the case of the L65M mutant the yield of photoproduct formation is similar to the wild type protein, but CO recombination is faster (k = 1764 s^{-1}). The L65T protein shows low photoproduct yield at 6 μs (29%) and also fast CO recombination (k = 2929 s^{-1}). The fast recombination rates in both mutants implies significant role of L65 in controlling the ligand dynamics. The data on the Y43 mutants demonstrate that the rate of recombination (k = 285 s^{-1}-820 s^{-1}) is mutant dependent and a higher barrier to recombination is formed in the case of the Y43A mutant. The Y43A mutant protein exhibited very low O_2 affinity and the Fe(II)-O_2 complex was not detected in the RR spectrum,[3] but in the case of the CO binding, the frequency of CO, the photodissociation yield, and the rebinding constant are similar to that of the wild type. Furthermore, the kinetic analysis for the amide I and heme propionate(s) modes in the Y43A mutant (Figure 4S, ESI) reveals a similar behaviour with the wild type protein; the protein relaxation and heme propionates perturbation correlate with CO recombination. The photoproduct yield for the CO adduct of Y43F (34%) is significantly lower compared to the wild type. It should be noted that in the Y43F mutant, both the Fe(II)-CO and Fe(II)-O_2 frequencies were different compared to those of the wild type, indicating that Y43 makes a H-bond with both the O_2 and CO ligands.[3] On the other hand, the Y43W mutant exhibited very high (>150 s^{-1}) O_2 dissociation constant and the Fe(II)-O_2 complex was not detected.[3] In the case of the CO-bound Y43W mutant, the CO frequency is 9 cm^{-1} lower than the wild type, high photoproduct yield is observed, but the recombination rate is higher than that observed in the wild type.

In YddV-heme the mutation of L65 to either Met (a residue of similar size and hydrophobicity) or Thr (a polar residue) results in significantly faster CO recombination rates compared to that observed for the wild type protein, even though the ν(CO) is not affected in the L65T mutant. Therefore, our data suggest that L65 is an important part of the kinetic barrier to ligand rebinding and no correlation between ν(CO) and the recombination rate is observed. Interestingly, the corresponding Leu residue in HemAT (L92) has been proposed to act as part of the conformational gate for ligand access in the heme pocket, based on the low photoproduct yield observed for L92 mutants in continuous wave photolysis experiments; however, kinetic measurements were not performed.[29] The mutation of Y43 to Ala, an apolar residue with less steric hindrance than Tyr, creates a higher burrier to CO recombination compared to the wild type protein and the Y43F and Y43W mutants. This appears to be a contradictory observation, since the expected increased available space in the heme pocket in the Y43A mutant compared to wild type YddV-heme and the Y43F and Y43W mutants would predict an increase in the rate of CO recombination.[21] The diverse effects of Y43 mutations on the CO recombination rate are challenging to interpret in the absence of a crystal structure of YddV that would allow the identification of possible interactions of Y43 with other distal site residues and/or internal water solvent molecule(s), which ultimately affect the rate of CO recombination and result in its decrease in the Y43A mutant. Taken together, the inspection of the CO recombination rates and the absence of the minor H-bonded conformer in the YddV-heme mutants suggest strong coupling of the L65 and Y43 residues to the properties of the bound CO to the heme iron. The comparison of the O_2 and CO data demonstrate that L65 and Y43 are crucial for ligand recognition and discrimination, and thus for specific sensing of gases.[3,19]

The following discussion compares the behavior of the distal residues Y43 and L65, the role of the heme propionates and protein backbone relaxation observed in YddV-heme-CO experiments to the corresponding features of the well-studied GCS protein HemAT. In comprehensive studies of HemAT, the unique specificity and tuning of the distal amino acid residues in constructing the necessary conformational changes towards ligand recognition were demonstrated. The behavior of T95 and Y70 upon binding of O_2, CO, and NO to the heme iron produced distinct ligand-bound conformations, indicating that these residues are the major contributors towards ligand recognition and discrimination, and L92 induced the necessary structural changes to T95 and Y70 to maintain the H-bonded conformers.[15,28] Such specific recognition and discrimination of iron bound gaseous ligands by the distal protein environment is crucial to the intramolecular signal transduction by HemAT. For the signal transduction mechanism in HemAT the G, H and B helices undergo significant displacement upon ligand binding that has been suggested to trigger conformational changes from the sensor domain to the function domain.[8,18,33] In YddV, the crucial residues in the recognition of the O_2- and CO-bound to the heme iron are L65 and Y43 that facilitate the formation of H-bonded conformers; when those residues are mutated the H-bonded closed conformer of the heme-CO adduct is absent. The overall distal moiety dynamics of the heme in YddV appears quite distinct from that of HemAT. In HemAT, the sensor domain displayed a signal for the amide I vibration in the UV RR spectra in hundreds of nanoseconds subsequent to CO photolysis and recovery in 50 μs, indicating that the isolated sensor domain undergoes fast conformational changes of the protein backbone upon CO photolysis.[33] In YddV-heme the relaxation of the amide vibration is completed with a rate constant of 480 s^{-1} that is similar with the rebinding of CO (k = 528 s^{-1}) indicating a much slower process for conformational relaxation of the protein compared to HemAT. Such protein dynamics in HemAT has been proposed to play a crucial role in the signaling process. In HemAT it has been shown that upon O_2 binding to the heme a H-bond forms between H86 and the heme propionate, therefore inducing a conformation change that is communicated to the CE loop and the E-helix.[16,18] This conformational change is regarded as essential for signal transduction on HemAT. Hydrogen bonding networks that include the heme propionates and are essential for transmitting the CO/NO/O_2 binding signals from the heme to the protein have also been identified in myoglobin.[34] We observe conformational changes of the protonated and deprotonated forms of the heme propionates in YddV-heme upon CO photodissociation, suggesting that the heme propionates may be important in communicating changes from the heme to the protein in YddV, similarly to HemAT.

Conclusions

In summary, our results demonstrate a significant role for L65 and Y43 in controlling the properties of the heme-bound ligand and ligand dynamics in YddV. Taken together, our results and those previously reported, show that there are distinct differences in the interaction of YddV with CO and O_2 as compared to the well-studied sensor protein HemAT, and that protein conformational changes upon ligand dissociation and rebinding are slower for YddV. Of particular interest is the role of the heme propionates in both YddV and HemAT. The heme propionates appear to behave in a similar way in both proteins upon ligand binding/dissociation. Experiments on the YddV-O_2 adduct are underway to further explore the heme-protein communication pathway and the mechanism of intramolecular signal transduction.

Acknowledgments

This work was funded by the European Regional Development Fund and the Republic of Cyprus through the Research Promotion Foundation (Grants ANAVATHMISI/PAGIO/0308/14 and PENEK/0609/41) and University of Cyprus internal grant to EP, and the Charles University in Prague (UNCE 204025/2012), Grant Agency of Charles University in Prague (756214) and the Grant Agency of the Czech Republic (grant 15-19883S) to MM.

Notes and references

[a] Department of Chemistry, University of Cyprus, PO Box 2037, 1678 Nicosia, Cyprus. E-mail: effiep@ucy.ac.cy.
[b] Department of Biochemistry, Faculty of Science, Charles University in Prague, 128 43 Prague 2, Czech Republic.
Electronic Supplementary Information (ESI) available: Figures S1, S2, S3, S4 and Table S1. See DOI: 10.1039/b000000x/

1 M. M. Méndez-Ortiz, M. Hyodo, Y. Hayakawa and J. Membrillo-Hernádez, Genome-Wide Transcriptional Profile of *Escherichia coli* in Response to High Levels of the Second Messenger 3′,5′-Cyclic Diguanylic Acid, *J. Biol. Chem.*, **281**, 8090-8099.

2 J. R. Tuckerman, G. Gonzalez, E. H. S. Sousa, X. Wan, J. A. Saito, M. Alam and M-A. Gilles-Gonzalez, An Oxygen-Sensing Diguanylate Cyclase and Phosphodiesterase Couple for c-di-GMP Control, *Biochemistry*, 2009, **48**, 9764–9774.

3 K. Kitanishi, K. Kobayashi, Y. Kawamura, I. Ishigami, T. Ogura, K. Nakajima, J. Igarashi, A. Tanaka and T. Shimizu, Important Roles of Tyr43 at the Putative Heme Distal Side in the Oxygen Recognition and Stability of the Fe(II)-O_2 Complex of YddV, a Globin-Coupled Heme-Based Oxygen Sensor Diguanylate Cyclase, *Biochemistry*, 2010, **49**, 10381-10393.

4 M. Martínková, K. Kitanishi and T. Shimizu, T., Heme-based Globin-Coupled Oxygen Sensors: Linking Oxygen to Functional Regulation of Diguanylate Cyclase, Histidine Kinase, and Methyl-Accepting Chemotaxis, *J. Biol. Chem.*, 2013, **288**, 27702-27711.

5 Y. Sasakura, T. Yoshimura-Suzuki, H. Kurokawa and T. Shimizu, Structure-Function Relationships of *Ec*DOS, a Heme-Regulated Phosphodiesterase from *Escherichia coli*, *Acc. Chem. Res.* **39**, 37-43.

6 A. Moglich, R. A. Ayers and K. Moffat, Structure and Signalling Mechanism of Per-ARNT_Sim Domains, *Structure*, **17**, 1282-1294.

7 S. Hou, R. W. Larsen, D. Boudko, C. W. Riley, E. Karatan, M. Zimmer, G. W. Ordal and M. Alam, Myoglobin-like Aerotaxis Transducers in Archaea and Bacteria, *Nature*, 2000, **403**, 540-547.

8 W. Zhang and G. N. Jr. Phillips, Structure of the Oxygen Sensor in *Bacillus subtilis*: Signal Transduction of Chemotaxis by Control of Symmetry, *Structure*, 2003, **11**, 1097-1110.

9 X. Wan, J. R. Tuckerman, J. A. Saito, T. A. K. Freitas, J. S. Newhouse, J. R. Denery, M. Y. Galperin, G. Gonzalez, M. A. Gilles-Gonzalez and M. Alam, Globins Synthesize the Second Messenger Bis-(3′–5′)-Cyclic Diguanosine Monophosphate in Bacteria, *J. Mol. Biol.*, 2009, **388**, 262-270.

10 H. Sawai, S. Yoshioka, T. Uchida, M. Hyodo, Y. Hayakawa, K. Ishimori and S. Aono, Molecular Oxygen Regulates the Enzymatic Activity of a Heme-Containing Diguanylate Cyclase (HemDGC) for the Synthesis of Cyclic di-GMP, *Biochim. Biophys. Acta – Proteins and Proteomics*, 2010, **1804**, 166-172.

11 L. Thijs, E. Vinck, A. Bolli, F. Trandafir, X. Wan, D. Hoogewijs, M. Coletta, A. Fago, R. E. Weber, S. Van Doorslaer, P. Ascenzi, M. Alam, L. Moens and S. Dewilde, Characterization of a Globin-Coupled Oxygen Sensor with a Gene-Regulating Function,. *J. Biol. Chem.*, 2007, **282**, 37325-37340.

12 A. Pesce, L. Thijs, M. Nardini, F. Desmet, L. Sisinni, L. Gourlay, A. Bolli, M. Coletta, S. Van Doorslaer, X. Wan, M. Alam, P. Ascenzi, L. Moens, M. Bolognesi, S. Dewilde, HisE11 and HisF8 Provide Bis-histidyl Heme Hexa-Coordination in the Globin Domain of *Geobacter sulfurreducens* Globin-Coupled Sensor, *J. Mol. Biol.*, 2009, **386**, 246-260.

13 K. Kitanishi, K. Kobayashi, T. Uchida, K. Ishimori, J. Igarashi and T. Shimizu, Identification and Functional and Spectral Characterization of a Globin-coupled Histidine Kinase from *Anaeromyxobacter* sp. Fw109-5, *J. Biol. Chem.*, 2011, **286**, 35522-35534.

14 R. Hengge, Principles of c-di-GMP Signalling in Bacteria, *Nat. Rev. Microbiol.*, 2009, **7**, 263-273.

15 T. Ohta, H. Yoshimura, S. Yoshioka, S. Aono and T. Kitagawa, Oxygen Sensing Mechanism of HemAT from *Bacillus subtilis*: A Resonance Raman Spectroscopic Study, *J. Am. Chem. Soc.*, 2004, **126**, 15000-15001.

16 H. Yoshimura, S. Yoshioka, K. Kobayashi, T. Ohta, T. Uchida, M. Kubo, T. Kitagawa and S. Aono, Specific Hydrogen-Bonding Networks Responsible for Selective O_2 Sensing of the Oxygen Sensor Protein HemAT from *Bacillus subtilis*, *Biochemistry*, 2006, **45**, 8301-8307.

17 W. Zhang, J. S. Olson and G. N. Jr. Phillips, Biophysical and Kinetic Characterization of HemAT, an Aerotaxis Receptor from *Bacillus subtilis*, *Biophys. J.*, 2005, **88**, 2801-2814.

18 S. F. El-Mashtoly, Y. Gu, H. Yoshimura, S. Yoshioka, S. Aono and T. Kitagawa, Protein Conformational Changes of HemAT-*Bs* upon Ligand binding Probed by Ultraviolet Resonance Raman Spectroscopy, *J. Biol. Chem.*, 2008, **283**, 6942-6949.

19 N. Nakajima, K. Kitanishi, K. Kobayashi, N. Kobayashi, J. Igarashi and T. Shimizu, Leu65 in the Heme Distal Side is Critical for the Stability of the Fe(II)-O_2 Complex of YddV, a Globin-Coupled Oxygen Sensor Diguanylate Cyclase, *J. Inorg. Biochem.*, 2012, **108**, 163-170.

20 M. Stranava, M. Martínková, M. Stiborová, P. Man, K. Kitanishi, L. Muchová, L. Vítek, V. Martínek and T. Shimizu, Introduction of Water into the Heme Distal Side by Leu65 Mutations of an Oxygen Sensor, YddV, Generates Verdoheme and Carbon Monoxide, Exerting the Heme Oxygenase Reaction, *J. Inorg. Biochem.*, 2014, **140**, 29-38.

21 T. Li, M. L. Quillin, G. N. Jr. Phillips and J. S. Olson, Structural Determinants of the Stretching Frequency of CO Bound to Myoglobin, *Biochemistry*, 1994, **33**, 1433-1446.

22 K. Gerwert, *Infrared and Raman Spectroscopy of Biological Materials*, Marcel Dekker, NY, 2000, ch. 6, pp.193-231.

23 D. Heibrink, H. Sigurdson, C. Bolwien, P. Brzezinski and J. Heberle, Transient Binding of CO to Cu_B in Cytochrome *c* Oxidase Is Dynamically Linked to Structural Changes around a Carboxyl Group: A Time-Resolved Step-Scan Fourier Transform Infrared Investigation, *Biophys. J.*, 2002, **82**, 1-10.

24 K. Koutsoupakis, S. Stavrakis, E. Pinakoulaki, T. Soulimane and C. Varotsis, C. "Direct Observation of the Equilibrium Cu_B-CO Complex and Functional Implications of the Transient Heme a_3 Propionates in Cytochrome ba_3-CO from *Thermus thermophilus*: FTIR and Time-Resolved Step-Scan FTIR Studies, *J. Biol. Chem.*, 2002, **277**, 32860-32866.

25 C. Koutsoupakis, E. Pinakoulaki, S. Stavrakis, V. Daskalakis and C. Varotsis, Time-resolved Step-Scan Fourier Transform Infrared Investigation of Heme-Copper Oxidases: Implications for O_2 Input and H_2O/H^+ Output Channels, *Biochim. Biophys. Acta-Bioenergetics*, 2004, **1655**, 347-352.

26 Pinakoulaki, E.; Varotsis, C. Time-Resolved Resonance Raman and Time-Resolved Step-Scan FTIR Studies of Nitric Oxide Reductase from *Paracoccus denitrificans*: Comparison of the Heme b_3-Fe_B Site to that of the Heme-Cu_B in Oxidases. *Biochemistry* **2003**, *42*, 14856-14861.

27 E. Pinakoulaki, C. Koutsoupakis, H. Sawai, A. Pavlou, Y. Kato, Y. Asano and S. Aono, Aldoxime Dehydratase: Probing the Heme Environment Involved in the Synthesis of the Carbon-Nitrogen Triple Bond, *J. Phys. Chem. B*, 2011, **115**, 13012-13018.

28 E. Pinakoulaki, H. Yoshimura, S. Yoshioka, S. Aono and C. Varotsis, Recognition and Discrimination of Gases by the Oxygen-Sensing Signal Transducer Protein HemAT as Revealed by FTIR Spectroscopy, *Biochemistry*, 2006, **45**, 7763-7766.

29 E. Pinakoulaki, H. Yoshimura, V. Daskalakis, S. Yoshioka, S. Aono and C. Varotsis, Two Ligand Binding Sites in the O_2-Sensing Signal Transducer HemAT: Implications for Ligand Recognition/Discrimination and Signaling, *Proc. Natl. Acad. Sci. USA*, 2006, **103**, 14796-14801.

30 A. Barth, Infrared Spectroscopy of Proteins. *Biochim. Biophys. Acta*, 2007, **1767**, 1073-1101.

31 J. Behr, P. Hellwig, W. Mantele and H. Michel, Redox Dependent Changes at the Heme Propionates in Cytochrome *c* Oxidase from *Paracoccus denitrificans*: Direct Evidence from FTIR Difference Spectroscopy in Combination with Heme Propionate ^{13}C Labeling, *Biochemistry*, 1998, **37**, 7400-7406.

32 C. Koutsoupakis, T. Soulimane and C. Varotsis, Probing the Q-Proton Pathway of ba_3-Cytochrome *c* Oxidase by Time-Resolved Fourier Transform Infrared Spectroscopy, *Biophys. J.*, 2004, **86**, 2438- 2444.

33 S. F. El-Mashtoly, M. Kubo, Y. Gu, H. Sawai, S. Nakashima, T. Ogura, S. Aono and T. Kitagawa, Site-Specific Protein Dynamics in Communication Pathway from Sensor to Signaling Domain of Oxygen Sensor Protein HemAT-*Bs*, *J. Biol. Chem.*, 2012, **287**, 19973-19984.

34 Y. Gao, S. F. El-Mashtoly, B. Pal, T. Hayashi, K. Harada and T. Kitagawa, Pathway of Information Transmission from Heme to Protein upon Ligand Binding/Dissociation in Myoglobin Revealed by UV Resonance Raman Spectroscopy, *J. Biol. Chem,*. 2006, **281**, 24637-24646.